CANMET

REPORT 80-16E

Canada Centre for Mineral and Energy Technology

Centre canadien de la technologie des minéraux et de l'énergie

SYNTHESIS AND CHARACTERIZATION OF POTASSIUM ION CONDUCTORS IN THE SYSTEM K_2O-Al_2O_3-TiO_2

D.H.H. QUON AND T.A. WHEAT

ENERGY RESEARCH PROGRAM
MINERAL SCIENCES LABORATORIES

Energy, Mines and Resources Canada
Énergie, Mines et Ressources Canada

MAY 1980

Available in Canada through

Authorized Bookstore Agents
and other bookstores

or by mail from

Canadian Government Publishing Centre
Supply and Services Canada
Hull, Quebec, Canada K1A 0S9

CANMET
Energy, Mines and Resources Canada,
555 Booth St.,
Ottawa, Canada K1A 0G1

or through your bookseller

Catalogue No. M38–13/80-16E
ISBN: 0-660-10747-3

Canada: $2.50
Other countries: $3.00

Price subject to change without notice.

En vente au Canada par l'entremise de nos

agents libraires agréés
et autres librairies

ou par la poste au:

Centre d'édition du gouvernement du Canada
Approvisionnements et Services Canada
Hull, Québec, Canada K1A 0S9

CANMET
Énergie, Mines et Resources Canada,
555, rue Booth
Ottawa, Canada K1A 0G1

ou chez votre libraire.

Nº de catalogue M38–13/80-16E
ISBN: 0-660-10747-3

Canada: $2.50
Hors Canada: $3.00

Prix sujet à changement sans avis préalable.

SYNTHESIS AND CHARACTERIZATION OF POTASSIUM ION CONDUCTORS IN THE SYSTEM K_2O-Al_2O_3-TiO_2

by

D.H.H. Quon* and T.A. Wheat*

ABSTRACT

The present work forms part of a program to develop ionically conducting materials for potential use in energy storage and conversion systems. With applications in high energy-density batteries, fuel cells and sensors, such materials are expected to play an increasingly important role in the future development of energy management systems.

Of the more than 30 known solid-state ionically conducting materials, those having compositions in the K_2O-Al_2O_3-TiO_2 system are reported to have electrical properties that only barely meet requirements for battery applications. However, the limited data available have been generated using relatively poor quality specimens produced from ball-milled material, whereas it is important for potential applications to establish the true intrinsic properties. For that purpose high-quality sintered bodies are required, and hence a wet-chemical process was developed that resulted in the synthesis of homogeneous, reactive raw materials that could be sintered to high density.

A series of compositions having the general formula $K_xAl_xTi_{8-x}O_{16}$ was prepared in which $1.6 < x < 1.9$, using both nitrate- and acetate-based dopants. It has been established that these compositions yield single-phase products when x lies between 1.6 and 1.9. At high titania contents, in which x is less than 1.6, rutile is precipitated whereas at low titania concentrations a new phase that is isostructural with $K_3Ti_6O_{13}$ is formed.

---

*Research scientist, Ceramics Section, Mineral Processing Laboratory, Mineral Sciences Laboratories, CANMET, Energy, Mines and Resources Canada, Ottawa.

SYNTHESE ET CHARACTERIZATION DES CONDUCTEURS D'ION DE POTASSIUM DANS LE SYSTEME K_2O-Al_2O_3-TiO_2

par

H.H. Quon* et T.A. Wheat*

RESUME

Le présent rapport fait partie intégrante d'un programme de perfectionnement des matériaux conducteurs ioniques susceptibles d'être employés pour l'emmagasinage de l'énergie et les systèmes de conversion d'énergie. On prévoit que de tels matériaux joueront un rôle de plus en plus important dans les travaux de perfectionnement à venir des systèmes d'exploitation d'énergie, ceux-ci ayant en plus des applications dans les piles à haute densité, les piles à combustibles et les détecteurs.

Des 30 matériaux conducteurs ioniques à l'état solide connus, on a signalé que ceux qui possèdent des compositions dans le systéme K_2O-Al_2O_3-TiO_2 ont des propriétés électriques qui rencontrent seulement à peine les conditions d'applications à la pile électrique. Cependant, le petit nombre de données disponibles a été obtenu en se servant d'une qualité relativement pauvre de spécimens produits de matériaux broyés à boulets, tandis qu'il importe à l'évaluation des applications éventuelles d'établir les propriétés intrinsèques véritables. Dans ce but des corps frittés de haute qualité sont requis, et d'où un procédé chimique par voie humide fut développé qui aboutit à la synthèse de matières brutes, homogènes et réactives capables d'être agglomerées par frittage jusqu'à haute densité.

On a préparé une série de compositions dont la formule générale est $K_xAl_xTi_{8-x}O_{16}$ et dans laquelle $1.6<x<1.9$, en utilisant des dopants à base de nitrate et d'acétate. Il a été établi que ces compositions rendent des produits monophasés quand x réside entre 1.6 et 1.9. A une haute teneur en titane, dans lequel x est moindre que 1.6, le rutile est précipité tandis qu'à des concentrations faibles en titane on remarque la formation d'une nouvelle phase qui est isostructurale accompagné de $K_3Ti_6O_{13}$.

*Chercheur scientifique, Section de la céramique, Laboratoire de traitement des minéraux, Laboratoires des sciences minérales, CANMET, Energie, Mines et Ressources Canada, Ottawa.

CONTENTS

TABLES

FIGURES

INTRODUCTION

Although the mineral hollandite (Ba-substituted alpha-MnO_2) and structurally related materials have been known for some time, it was only recently recognized that materials isostructural with hollandite were effective cationic conductors. These materials crystallize in the tetragonal system and form tunnels in the c-direction through which group I or group II cations may move under an applied chemical or electrical potential.

At present, there are more than 30 known solid-state electrolytes and most of these are conductive to the elements of group IA of the Periodic Table (1). Although the first indication of ionic conductivity in a material isostructural with hollandite was obtained in 1958 (2), there has been only a limited number of investigations of structurally related materials. The two hollandites: $K_xAl_xTi_{8-x}O_{16}$ and $K_xMg_{x/2}Ti_{8-x/2}O_{16}$ have been studied by Takahashi, Kuwabara, Reau, Singer and co-workers (3-6). These investigators showed these materials have an ac conductivity of $\sim 10^{-2}$ $(\Omega.cm)^{-1}$. However, the electrical data were obtained from materials synthesized by a conventional ball-milling technique. In a previous report by the present authors on the fabrication of hollandites having the general composition: $K_xMg_{x/2}Ti_{8-x/2}O_{16}$, it was demonstrated that such ball-milled materials only sintered to 90% of the theoretical density whereas materials prepared using a wet-chemical process sintered to >95% (7). In addition, microstructural analyses demonstrated the development of second-phase materials in sintered samples produced using ball-milled raw materials.

Because of the known sensitivity of ionic conductivity to significant impurity levels and the development of inhomogeneities, it was decided to avoid ball milling as a means of mixing the raw materials and instead, to develop a wet-chemical process that combined the virtues of sol-gel processing with freeze drying so that reactive and homogeneous raw materials could be produced. In essence, the method exploits the homogeneity developed in a doped sol-gel slurry and which is captured by very rapid spray freezing followed by freeze drying.

EXPERIMENTAL PROCEDURE

Materials in the K_2O-Al_2O_3-TiO_2 system were prepared by a wet-chemical process that yielded fired compositions having the general formula: $K_xAl_xTi_{8-x}O_{16}$ in which x was between 1.6 and 1.9. The process is similar to that developed earlier by the present authors for the synthesis of reactive materials in the K_2O-MgO-TiO_2 system (7).

Two series of materials were prepared in this study, based on the use of water-soluble nitrates and on soluble acetates respectively. In both cases, the procedure involved the doping of a washed $Ti(OH)_4$ precipitate with a solution containing dissolved K and Al salts. Thereafter, the continuously agitated mixture was sprayed directly into liquid N_2 to capture the homogeneity of the slurry in the solid state by flash freezing very small droplets of material. The product was finally freeze dried to produce a white, essentially free-flowing powder. A general outline of the process is given in Fig. 1 and 2.

PRECIPITATION OF TITANIUM HYDROXIDE

The $Ti(OH)_4$ suspensions were obtained from 99.5% $TiCl_4$* using NH_4OH**. From the potentiometric titration data recorded earlier (7), the quantity and concentration of these two reagents required to fully precipitate the titanium component was already known.

To prepare $\sim$400 g of $Ti(OH)_4$, 391 mL (675 g) of $TiCl_4$ were first carefully diluted with 10 L of distilled water and this solution was then added slowly to a continuously stirred solution of 650 mL of as-received NH_4OH in 10 L of distil-

*Anachemia Chemicals Ltd., Toronto, Ontario (relative density 1.726)

**Allied Chemicals Ltd., Pointe Claire, Quebec (relative density 0.888)

led water. The pH of the suspension formed was adjusted to 6.5 by the addition of a minor amount of diluted NH_4OH and the slurry was made up to 50 L with additional distilled water. After standing overnight, during which the precipitate settled to ~13 L, i.e., a solids concentration of 2.18 *m* % (mass per cent), the clear supernatant liquor was discarded and replaced with distilled water. This washing process was continued until the $[Cl^-]$ in the stirred slurry was <20 μg/g.

After washing, the supernatant liquor was removed and the settled slurry stirred vigorously for 2 h prior to dividing it into approximately equal portions by transferring into pre-weighed containers. From duplicate gravimetric analyses of samples of the stirred $Ti(OH)_4$ slurry, the TiO_2 equivalent in each container was determined.

PREPARATION OF POTASSIUM- AND ALUMINUM-DOPED TITANATES

From the determination of the number of moles of TiO_2 equivalent in each container, the appropriate amount of either CH_3COOK and $(CH_3COO)_2(OH)Al.xH_2O$ or KNO_3 and $Al(NO_3)_3.9H_2O$ required to produce specific compositions was determined as shown in Appendix A.

In each case, the required amount of acetate or nitrate was dissolved in water to give a 0.5 molar solution, the K and Al salt solutions were then mixed and slowly added to rapidly stirred $Ti(OH)_4$ slurry. The resulting mixture was flash frozen by spraying directly into liquid N_2, using a doped slurry feed rate of 45 mL/min. The frozen material was finally freeze dried at -10°C for at least 48 h under a vacuum of 3.3 to 5.9 x 10^4 Pa (250 to 450 Torr) to produce a bulky and reactive hollandite precursor.

RESULTS AND DISCUSSION

CHARACTERIZATION OF AS-PREPARED RAW MATERIALS

Each composition of material prepared using either acetates or nitrates was examined using X-ray diffraction (XRD), thermogravimetric analysis (TGA) and differential thermal analysis (DTA) to determine the reaction sequences. Shrinkage during heating was observed using a Leitz heating microscope. For each analysis, standard procedures were used that have been reported elsewhere (7).

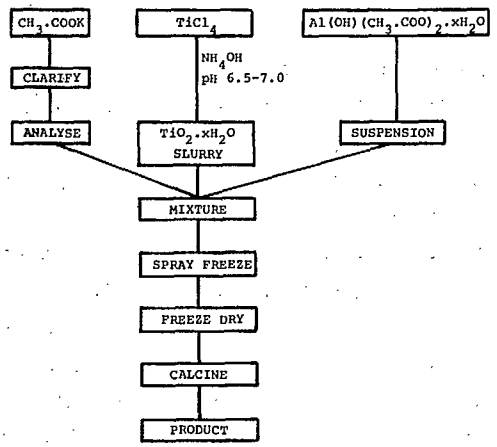

Fig. 1 - Flow sheet for the synthesis of materials in the K_2O-Al_2O_3-TiO_2 system using acetate-based dopants

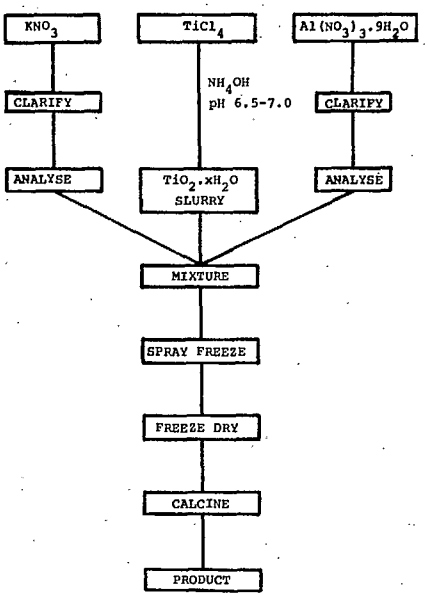

Fig. 2 - Flow sheet for the synthesis of materials in the K_2O-Al_2O_3-TiO_2 system using nitrate-based dopants

Thermal Analyses of Acetate-Doped Materials

Both DTA and TGA were obtained for a sample of undoped freeze-dried $Ti(OH)_4$. The DTA curve showed a broad endothermic peak between 80 and 250°C that was associated with a considerable mass loss of the sample and which was ascribed to the loss of physisorbed and chemisorbed water from the gel structure. At higher temperatures, a weak exothermic reaction recorded at 860°C was probably related to the rapid crystal growth of rutile, the high-temperature form of TiO_2.

The TGA curve obtained for $(CH_3COO)_2(OH)Al.xH_2O$ is given in Fig. 3 and shows that ∿20% mass loss occurs below 250°C. This loss was attributed to the removal first of physisorbed and subsequently of chemisorbed water. An additional ∿51% mass loss occurs between 250 and 400°C due to the progressive decomposition of the acetate and the formation of Al_2O_3. No further mass loss occurred with increasing temperature above 400°C. X-ray diffraction analyses of samples heated for 1 h between 100°C and 500°C indicated that only amorphous material was formed.

From the TGA curves of KNO_3 and $Al(NO_3)_3 \cdot 9H_2O$ shown in Fig. 4, it can be seen that

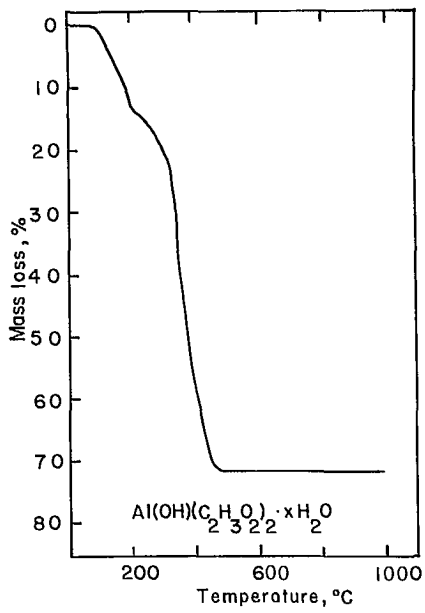

Fig. 3 - TGA curve of basic aluminum acetate heated in air at 6°C/min

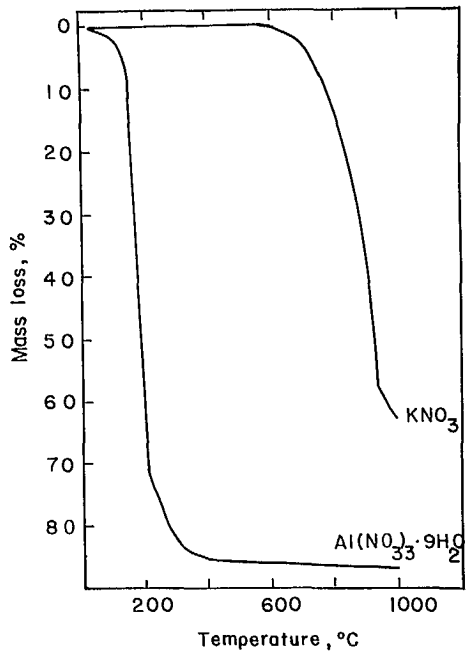

Fig. 4 - TGA curve of potassium and aluminum nitrates heated in air at 6°C/min

KNO_3 was stable up to ∿600°C; decomposition becomes appreciable above 800°C. Additional mass loss was recorded above 1000°C and was attributed to the volatilization of potassium oxide. In contrast to the relative stability of KNO_3, $Al(NO_3)_3 \cdot 9H_2O$ suffered a considerable mass loss at very low temperature: ∿72% loss occurred up to 210°C and a further 13% between 210 and 400°C. The considerable loss that occurred up to 210°C was due to the loss of water and the development of an anhydrous nitrate that decomposed to the oxide between 210 and 400°C.

The DTA and TGA data for the various compositions of acetate-based materials are shown in Fig. 5 and 6. Regardless of composition, DTA indicated an endothermic reaction at ∿180°C followed by a strong exothermic reaction at 400°C and a weak exotherm at ∿890°C. TGA indicated that a maximum mass loss of between 30 and 36% occurred below 400°C; no additional mass loss occurred at higher temperatures. The form of the DTA and TGA curves suggested that the powders lose water up to ∿180°C and at higher temperatures the loss was due to the decomposition of the potassium and alu-

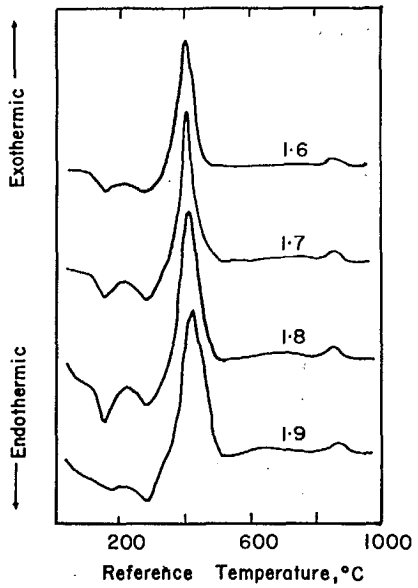

Fig. 5 - DTA curves for acetate-doped materials heated in air at 12°C/min

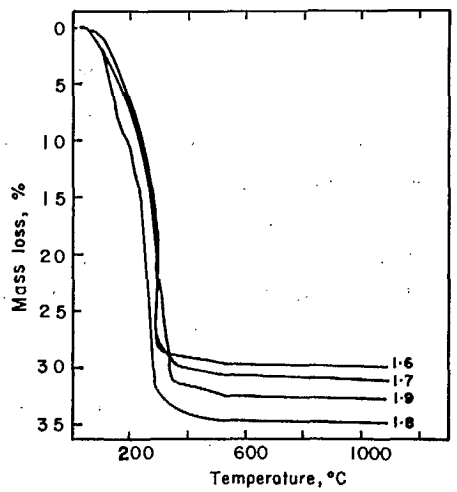

Fig. 6 - TGA curves for acetate-doped materials heated in air at 6°C/min

minum acetates. Although the exothermic reaction at ~400°C was not identified, it probably resulted from the formation of potassium oxalate from the acetate together with the crystallization of anatase, the low temperature form of TiO_2. The weak exotherm at ~850°C was assumed to result from the crystal growth of either hollandite or a metastable phase known to occur in this system.

To identify reactions suggested by the DTA data, samples of each composition were calcined for 1 h at temperatures just above and just below those recorded in DTA and were then analyzed by conventional XRD techniques.

X-ray Diffraction Analyses of Acetate-Doped Materials

The crystalline phases developed in calcined material were identified from Guinier-DeWolff diffraction patterns obtained using Fe-filtered CoK_α radiation. Figure 7 shows the diffractograms derived from a densitometer scan of the XRD pattern recorded on film as generated by various compositions of the acetate-based materials. It can be seen that very poorly crystalline material was obtained at temperatures below 700°C; at higher temperatures, well crystallized material was formed.

A phase analysis of calcined material shows that anatase and aluminum acetate were the first phases formed at temperatures below 300°C. At higher temperatures, the acetate was decomposed presumably to form an amorphous oxide and, at the same time, potassium oxalate crystallized to coexist with anatase up to ~500°C. It is probable that the exothermic peak recorded in DTA below 500°C was associated with the crystal growth of anatase and potassium oxalate. At 600°C, anatase reacted with the free potassium and aluminum salts to form a new compound that is isostructural with $K_3Ti_6O_{13}$. By 800°C, the free TiO_2 present had transformed from anatase to the high-temperature form of rutile, the $K_3Ti_6O_{13}$-type phase persisted and hollandite was first formed. At 900°C, it appeared that rutile reacted with the $K_3Ti_6O_{13}$-type material to form more hollandite; by 1000°C rutile had disappeared leaving only hollandite and the $K_3Ti_6O_{13}$-type material. A summary of this phase sequence is shown in Fig. 8.

Thermal Analyses of Nitrate-Doped Materials

The DTA and TGA data obtained for this series of materials are shown in Fig. 9 and 10. The TGA results show that there were two distinct

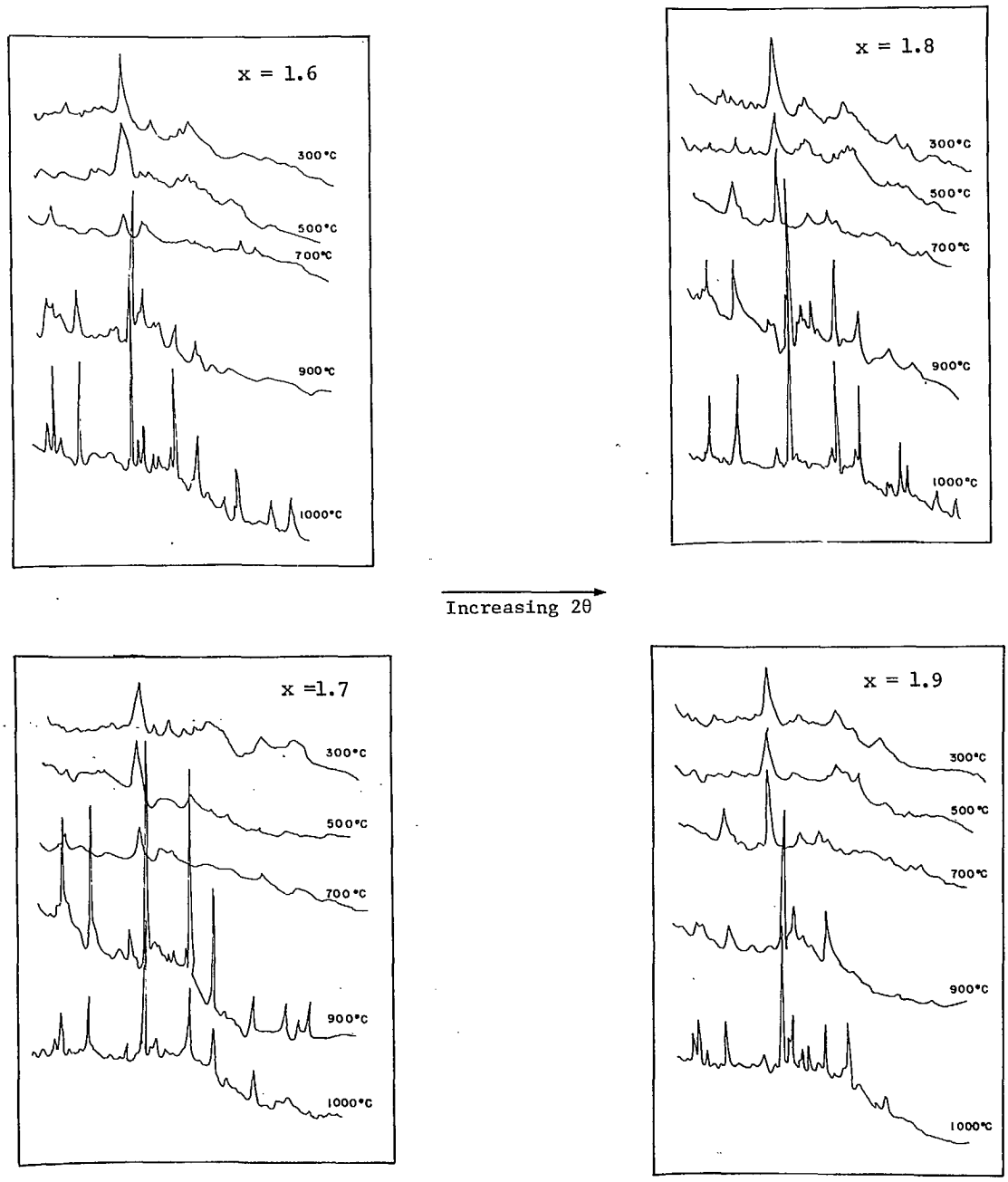

Fig. 7 - X-ray diffraction patterns of as-prepared acetate-doped materials after heating in air for 1 h at the temperatures indicated

regions of mass loss irrespective of composition. The first occurred at ∿200°C and the second at ∿650°C. The major mass loss at low temperatures was attributed to the progressive removal of physisorbed and then chemisorbed water from the $Ti(OH)_4$ component. Although the DTA trace recorded between 100 and 300°C did not reflect the progressive dehydration of the $Al(NO_3)_3.9H_2O$, it was assumed that the anhydrous nitrate phase was also formed over this temperature interval. The endo-

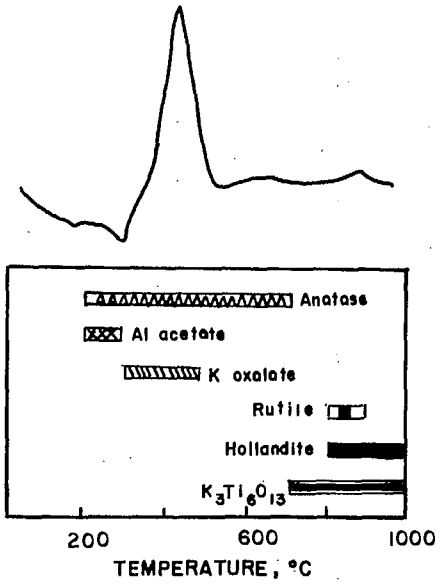

Fig. 8 - Summary of the reactions occurring during calcination in air of acetate-doped freeze-dried materials

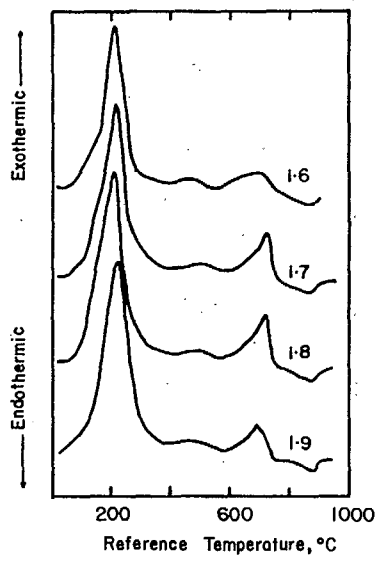

Fig. 9 - DTA curves for nitrate-doped materials heated in air at 12°C/min

thermic effects always associated with desorption processes were not recorded in the DTA due to the domination of a major exothermic reaction occurring at ∿210°C that probably resulted from the crystal growth of free TiO_2 as anatase.

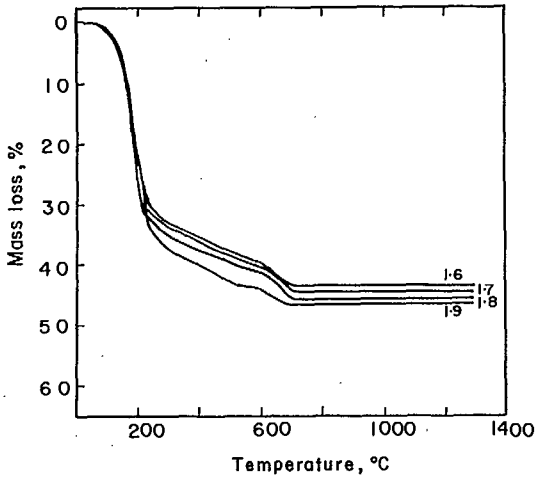

Fig. 10 - TGA curves for nitrate-doped materials heated in air at 6°C/min

The additional mass loss occurring above 200°C was ascribed to the progressive decomposition of the anhydrous potassium and aluminum salts present. The identity of the exothermic reaction at ∿700°C is unknown but it was possibly associated with the crystal growth of a $K_3Ti_6O_{13}$-type phase that was identified by XRD.

X-ray Diffraction Analyses of Nitrate-Doped Materials

The derived X-ray diffractograms obtained from densitometer scans of Guinier-DeWolff powder diffraction patterns of samples calcined in air for 1 h are shown in Fig. 11. In general, the behaviour of these materials was similar to that of the acetate-doped materials: poorly crystalline phases were developed below ∿700°C whereas well-crystallized products were obtained at higher temperatures.

The phase sequence developed in this series of raw materials was similar to that produced by the acetate-based powders. At low temperatures, crystalline KNO_3 was formed up to 300°C along with a poorly crystallized anatase from the chiefly amorphous as-dried powder. A $K_3Ti_6O_{13}$-type phase was first formed at 600°C; by 800°C,

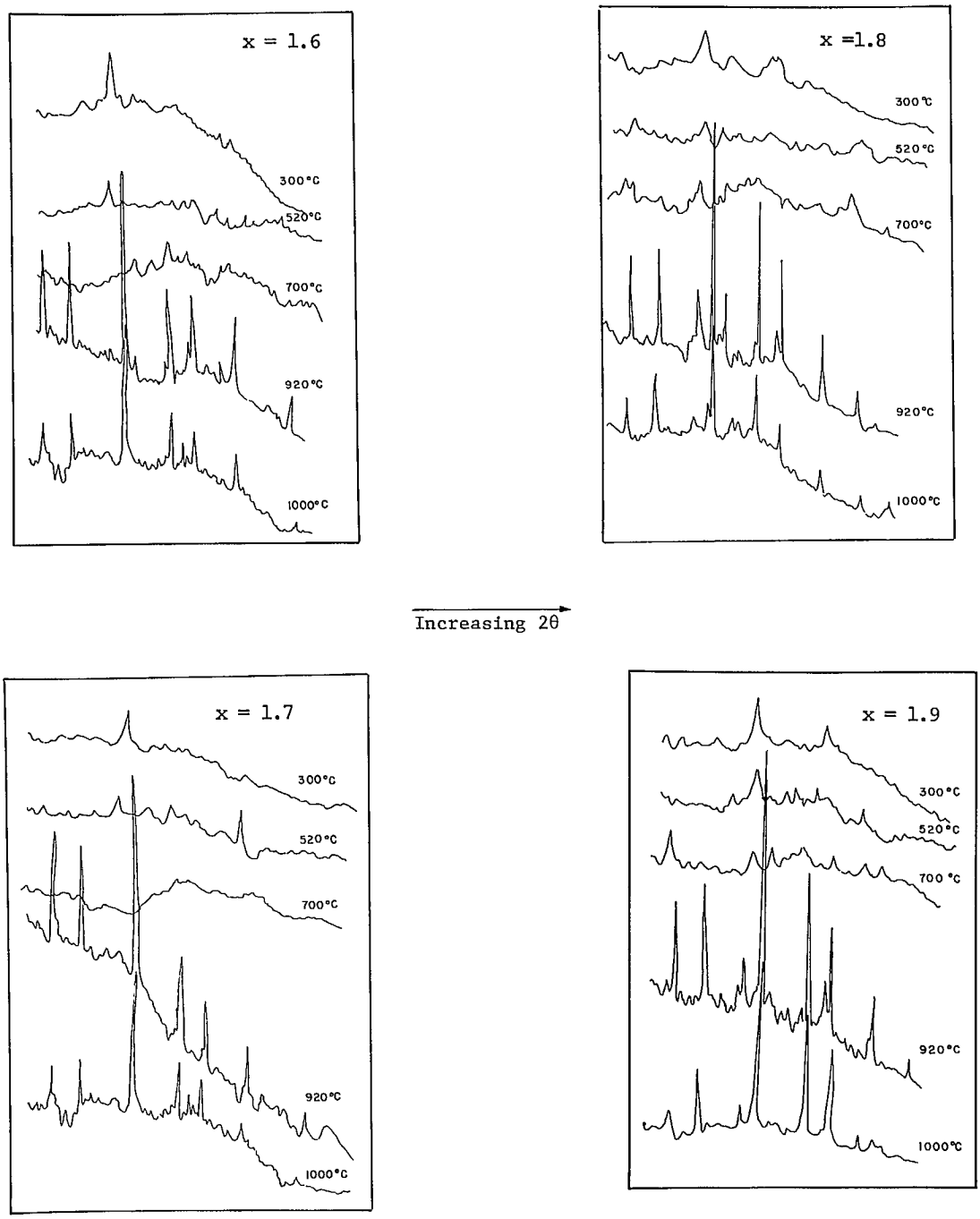

Fig. 11 - X-ray diffraction patterns of as-prepared nitrate-doped materials after heating in air for 1 h at the temperatures indicated

rutile and hollandite were also formed. At higher temperatures, the rutile began to react with the $K_3Ti_6O_{13}$-type phase forming more hollandite so that only hollandite and $K_3Ti_6O_{13}$-type material co-existed at 1000°C. A summary of this phase sequence is shown in Fig. 12.

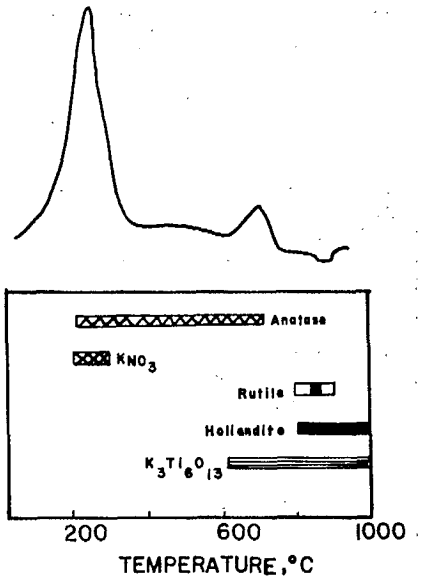

Fig. 12 - Summary of the reactions occurring during the calcination in air of nitrate-doped freeze-dried materials

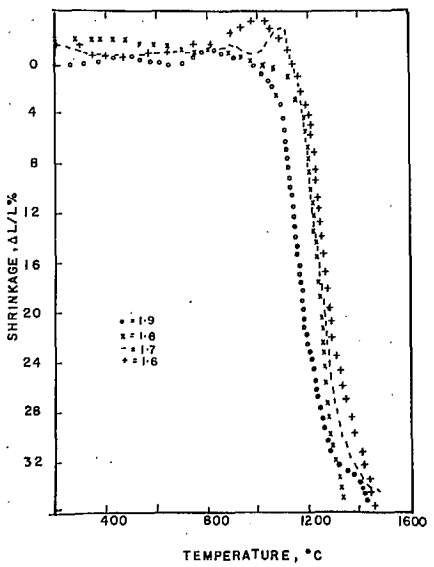

Fig. 13 - Typical sintering curves for the acetate-doped materials on heating in a static air atmosphere

Hot-Stage Optical Microscopy

This technique was used to determine the sintering characteristics of calcined samples having various compositions and drawn from the two basic series of materials studied. Each sample was first calcined in air for 1 h between 900 and 910°C prior to pressing into 3-mm cubes and examining in a Leitz heating microscope type IIA-P while heating at 6°C/min. At ∿100°C intervals, the projected image of the sample was photographically recorded as the temperature was raised to the desired value. From this series of photographs, the progressive shrinkage of each sample as a function of temperature was obtained. The data are shown in Fig. 13 and 14.

It can be seen that sintering started in both series of materials at ∿1000°C and became very rapid between 1200 and 1400°C. It is possible that the inflection in these curves at ∿1400°C resulted from the combined effects of a general reduction in the sintering rate together with an increase in the rate of volatilization of potassium oxide that led to a further volume shrinkage and a markedly non-stoichiometric product.

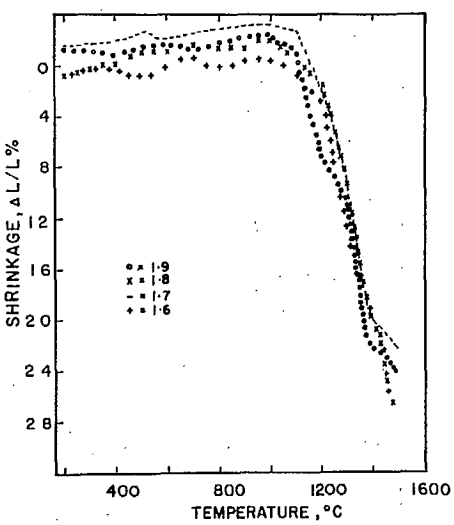

Fig. 14 - Typical sintering curves for the nitrate-doped materials on heating in a static air atmosphere

Although the general form of the curves is similar for each series of materials, a significant difference between the two types of raw materials was observed: the product of sintered acetate-doped powders was consistently grey when

heated above 1400°C, whereas the nitrate-based materials were always cream coloured after heating under the same conditions. Previous work had indicated that this colour change was related to a minor degree of non-stoichiometry developing as oxygen was lost from the system at high temperatures, and under deliberately strongly reducing firing conditions the fully reduced black products possessed a high degree of electronic conductivity (7). Because the present work was directed to the development of a series of solid-state electrolytes in which electronic conductivity must be minimized, efforts were subsequently made to ensure that only fully oxidized, cream-coloured sintered bodies were produced.

FABRICATION AND CHARACTERIZATION OF SINTERED MATERIALS

Prior to fabricating and sintering the as-prepared, freeze-dried powders, it was necessary to first calcine the materials to prereact the various components, remove the considerable amount of volatile material and reduce the degree of shrinkage and hence cracking that would otherwise occur during the sintering stage. The selection of the calcination temperature was necessarily a compromise between two competing requirements.

On the one hand, it was desirable to use a high temperature to ensure complete reaction and the development of the final phase assemblage. This would also ensure a much reduced firing shrinkage and the elimination of firing cracks. However, if too high a temperature were used it would lead to the vapourization of some of the potassium oxide, thereby giving non-stoichiometric compositions. In addition, an excessively high temperature would result in a marked reduction of the free surface area of the powder and hence the driving force for the subsequent densification of the compacted powder during sintering would be much reduced, preventing the development of a high sintered density.

On the other hand, if too low a calcination temperature were used it might be insufficient to ensure the complete decomposition of the components. In the present system, the retention of some of the acetate, nitrate or hydrated materials in compacted bodies would lead to a poor sintered density and possibly even the persistence of an open-pore structure. It would also allow an excessively high firing shrinkage and the certain development of firing cracks.

In the present materials, the extremes of the too high and too low calcination temperatures were ~1100°C, indicated by the firing curves, and ~750°C, suggested by both the DTA and XRD data. On this basis, 900°C was selected as the calcination temperature; this temperature was also found to be appropriate in the K_2O-MgO-TiO_2 system studied earlier by the authors (7).

Effect of Sintering Time and Temperature on Density

To determine the effect of temperature, a series of 1.25-cm dia discs of each composition was cold pressed under a uniaxial pressure of 70 MPa (10,000 psi) using powders calcined in air at 900°C for 1 h. These discs were fired in air at 1250, 1275, 1300 and 1325°C for 5 h.

The results, shown in Fig. 15 and 16, indicate that the densification of those materials in which $x > 1.7$ was optimized at a temperature of 1275°C irrespective of the dopants used to produce the initial powder. A temperature of 1275°C was also the optimum for the acetate-doped materials in which $x = 1.6$, but for nitrate-based powders of the same composition, the optimum sintering temperature was raised to 1325°C.

The effect of sintering time on the degree of densification of both types of powder was determined by firing a series of samples at 1275°C for various times. The results, shown in Fig. 17 and 18, indicated the optimum period to be between 3 and 5 h. However, the slight gain in density between 3 and 5 h noted could well be off-set by the greater loss of potassium oxide from the surface of samples sintered for the longer time. In addition, this slight gain might have been more apparent than real; because small samples were used to generate the data presented in Fig. 15 to 18 as the precision of the data was ±100 kg/m^3.

In an attempt to produce bigger samples and hence more precise density data and also to

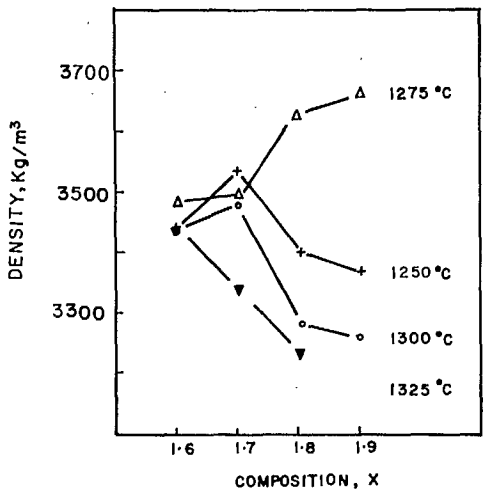

Fig. 15 - Variation of density with temperature for acetate-doped materials

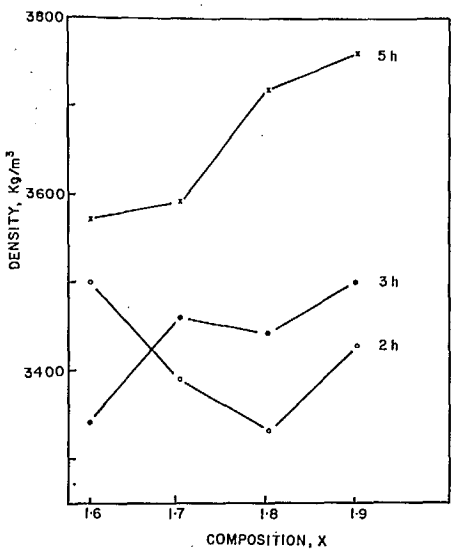

Fig. 17 - Variation of density with time of sintering acetate-based material at 1275°C

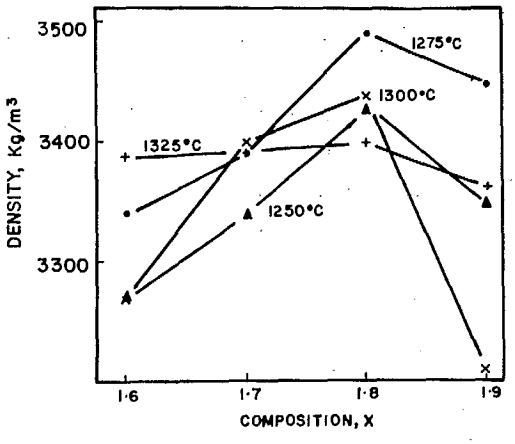

Fig. 16 - Variation of density with temperature for nitrate-doped materials

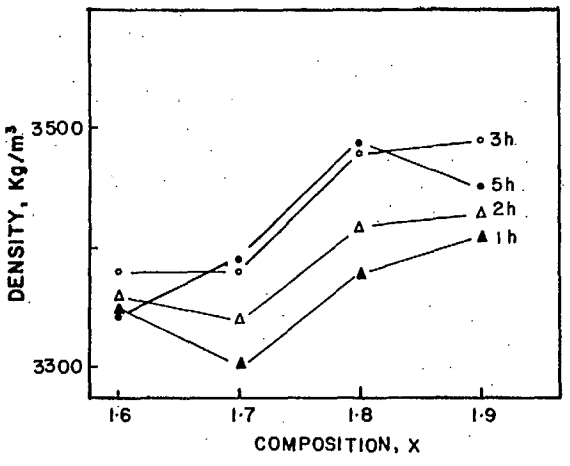

Fig. 18 - Variation of density with time of sintering nitrate-based material at 1275°C

produce samples suitable for electrical property studies, a series of both acetate- and nitrate-doped samples of all compositions was fabricated from calcined powders containing an added powder lubricant and binder. Because relatively small quantities of material were being handled, these organic additives were most conveniently distributed throughout each batch of powder by first dissolving 5 *m* % polyvinyl acetate* and 2 *m* % polyethylene glycol** in toluene and then spraying the mixture onto the surface of each composition.

*Gelva V-7, available from Monsanto Canada Ltd., Toronto

**Carbowax 400, available from Union Carbide Canada Ltd., Toronto

The powder was constantly turned and spread into a thin layer on a polyethylene sheet during this spraying stage until 15 *m* % of the mixture had been added to the powders of each composition. The solvent was then allowed to evaporate and the powder was transferred to a steel die and compacted uniaxially at 70 MPa (10 000 psi) to produce discs measuring 3.8 cm (1.5 in.) in diameter and 1 cm (0.45 in.) high. The samples were finally isostatically pressed at 210 MPa (30 000 psi).

It has been established in earlier work that the powder lubricant and binder used in the fabrication of the larger discs burned off in two stages and was eliminated from the ceramic at ∿420°C (7). Consequently, the discs were first heated to ∿500°C in a platinum-wound tube furnace using a slow heating rate of 1°C/min and held at that temperature for 16 h to ensure that all the organic additives had been fully oxidized and removed prior to sintering. Thereafter, the temperature was increased at 200°C/h up to the sintering temperature. The green and fired densities of bodies produced in this manner are given in Appendix A.

Effect of Furnace Atmosphere on Sintered Product

The initial firing of acetate-doped materials was conducted in a static air atmosphere. However, it was observed that in such samples having a composition in which x = 1.6 in which the TiO_2 concentration is high, a dark grey colour developed in contrast to the cream colour of samples in which x = 1.7 to 1.9. This darkening was attributed to reduction of the titanium in the sample; a similar effect was reported earlier for hollandites produced in the K_2O-MgO-TiO_2 system (7).

In an attempt to avoid this reduction of the TiO_2-rich compositions, discs were fired in a flowing wet O_2 atmosphere in a manner described earlier (7). Under these conditions, material having the composition x = 1.6 and prepared using acetates, developed a very light grey colour instead of the dark grey characteristic of sintering in a static air atmosphere. It has been pointed out by others that the use of citrates to prepare raw materials in other systems sometimes results in the retention of residual carbon in compacts during the firing cycle (8). In the present work, the use of organic additives to aid the fabrication of acetate-derived material offered an additional source for the formation of carbon during the calcination of the powder when access to oxygen was restricted in a static powder bed. Consequently, the titanium was reduced to Ti^{3+}.

Although not quite so sensitive, the nitrate-based materials containing an organic binder and lubricant, showed a similar effect in some cases, indicating that sufficient carbon to reduce the titanium would be produced by the incomplete pyrolysis of the additives. Without these organic additions, the nitrate-based powders developed a cream colour on firing in air, indicating a fully oxidized product.

Because of the success in producing oxidized material on firing in wet O_2, all subsequent samples for electrical characterization were produced by firing in this atmosphere. It was found adequate to use O_2 in the sintering cycle only at temperatures above 700°C on both the heating and cooling cycle. In practice, pure O_2 was bubbled through water held at 90°C to create O_2 atmosphere containing 45.66% water vapour; the gas velocity was adjusted to the cross section of the furnace so that a gas flux of 6 g/cm^2/h was maintained. Deviations from these conditions, such as the use of a lower gas flux or decreasing the moisture content of the O_2, invariably led to reduction of the TiO_2-rich compositions in which x = 1.6 and 1.7. Hence, the following conclusions may be drawn:

- the TiO_2-rich compositions of x = 1.6 can not be oxidized in a low flow rate of oxygen,
- as the TiO_2 content is lowered in the composition so the material is oxidized more readily,
- the use of organic additives to aid the development of high-density green pressed compacts can lead to the formation of carbon within the body during firing and hence to a reduction of the titanium components.

It can be seen from the data in Appendix A that there is a tendency for the sintered density to increase with an increasing amount of TiO_2 in the composition of the acetate-based mat-

erials. However, a high TiO_2 content also results in the production of partially reduced sintered materials, especially when x = 1.6. Although many sintering cycles were conducted with x = 1.6 acetate-based material under apparently fixed conditions, the state of oxidation of the product could never be assured. In one case, four discs produced from the same batch of powder and sintered at the same time produced three grey samples and one cream, the significant observation being that the cream disc was closest to the O_2 inlet and the darkest grey sample was furthest from the inlet. On other occasions, samples were produced that were partly cream and partly grey; in every case, the cream colour was developed in that part of the disc that contacted the saggers. Changing the composition of the sagger from 99.5% Al_2O_3 to Pt-coated furniture had no effect. Hence, it was concluded that the degree of oxidation that occurred in these marginal cases was not the result of a possible local composition change due to contact with the sagger, but resulted from the higher degree of gas turbulence that occurred at these points.

Microstructure of Sintered Materials

Samples of all compositions derived from both acetate- and nitrate-doped materials and fired at various temperatures were examined in reflected light using partially crossed polars to determine the grain size, microporosity and presence of any second phase. The technique for mounting and polishing these samples has been reported elsewhere (9).

Examination of the initially produced acetate-doped materials indicated that free TiO_2 was precipitated in the matrix of compositions in which x = 1.6 and 1.9. At that time, it was thought that the precipitate resulted from poor mixing of the acetate and $Ti(OH)_4$ due to the low solubility of $(CH_3COO)_2(OH)Al.xH_2O$. Hence, subsequent work concentrated on the more soluble nitrates for doping. However, the use of a nitrate-based material still resulted in the formation of TiO_2 precipitates in compositions having x = 1.9. These results are at variance with those of other workers who report that single-phase hollandites can be produced in the K_2O-Al_2O_3-TiO_2 system in the composition range $1.6 < x < 1.9$ (5). In the present work, single-phase material could only be produced in the range of x from 1.6 to less than 1.9. The difference may be due to the much longer sintering times employed elsewhere, which resulted in a substantial potassium loss and a shift in the phase boundaries as a new composition was formed.

Typical microstructures developed in the sintered acetate-based materials are shown in Fig. 19 to 22. It can be seen that there is a morphological difference between samples having high and low TiO_2 contents. In the former, in which x = 1.6, the crystal morphology is anhedral, but gradually becomes euhedral as the TiO_2 content is reduced so that at compositions in which x = 1.9 lath-shaped crystals are developed. The grain size also appears to increase with an increase in the TiO_2 content.

Figures 23 and 26 show typical microstructures developed in the nitrate-doped materials sintered under the same conditions. Similar morphological characteristics to those of the acetate-based samples can be observed. Examination of material in which x = 1.9 reveals the presence of second-phase TiO_2 in the matrix; this precipitate was formed in all samples of x = 1.9 sintered between 1250 and 1325°C. This is in contrast to the behaviour of material for which x = 1.6 and which had been sintered at 1275°C or lower where no TiO_2 precipitate was formed: only above 1275°C did this composition result in the formation of free TiO_2. This behaviour of precipitating TiO_2 in those compositions that have been sintered above 1275°C strongly suggests that the exsolution of TiO_2 from the matrix resulted from the progressive loss of potassium from the samples during the firing cycle and a shift in the composition from a single- to a two-phase field. The fact that second-phase TiO_2 was not observed in the acetate-doped materials when processed under similar conditions is not understood. The difference may be explained in part by the possible melting of the $Al(NO_3)_3 \cdot 9H_2O$ component in the freeze-dried powder during the initial stages of calcination, resulting in the development of inhomogeneity that persists throughout subsequent processing.

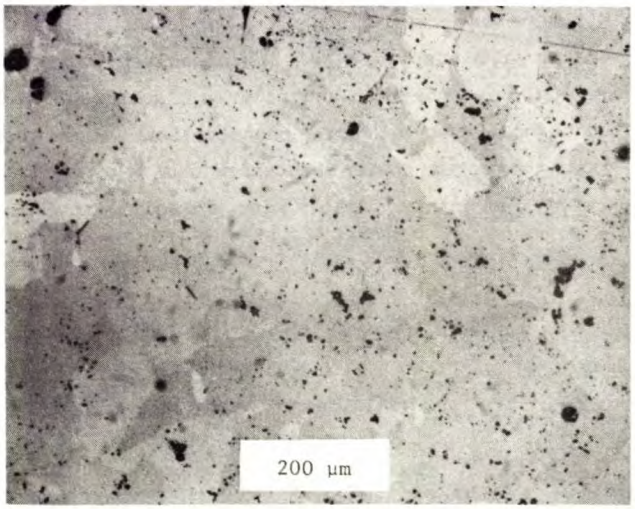

Fig. 19 - Microstructure developed in x = 1.6 acetate-doped material after firing at 200°C/h to 1275°C and holding at that temperature for 5 h

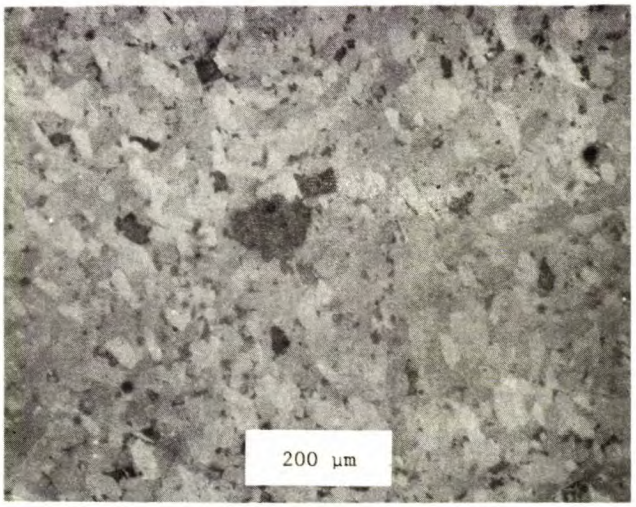

Fig. 21 - Microstructure developed in x = 1.8 acetate-doped material after firing at 200°C/h to 1275°C and holding at that temperature for 5 h

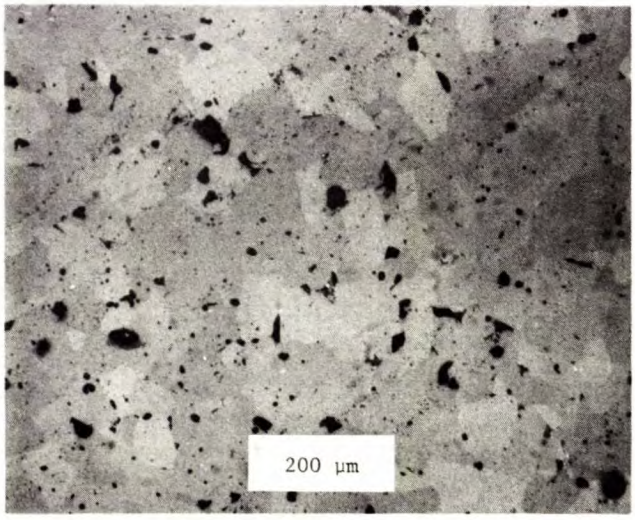

Fig. 20 - Microstructure developed in x = 1.7 acetate-doped material after firing at 200°C/h to 1275°C and holding at that temperature for 5 h

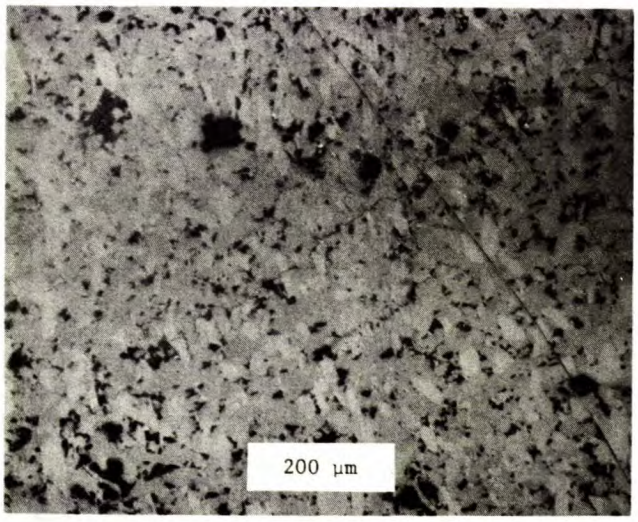

Fig. 22 - Microstructure developed in x = 1.9 acetate-doped material after firing at 200°C/h to 1275°C and holding at that temperature for 5 h

Both types of material shown in Fig. 19 to 26 were found to include isolated areas of macroporosity 15 to 25 µm in diameter throughout the microstructure. Consequently, subsequent samples were first milled to break up any agglomerates present and to simultaneously introduce powder lubricant and binder. In this manner, it was anticipated that the particle bridging that was probably occurring during the pressing stages, and which resulted in the voids seen in the sintered products, would be reduced or eliminated. Also, any degree of inhomogeneity developed in the ni-

trate-based materials would be removed at this stage.

After calcining in air at 900°C for 1 h, batches of each composition from both series of powders were milled in a rubber-lined container using 1.27-cm diameter high-alumina cylinders. Milling the powders slurried in methanol ensured the uniform dispersion of the dissolved polyethylene glycol lubricant and polyvinyl acetate binder throughout the powder; concentrations were such that the dried powder contained 5 *m* % binder and 2 *m* % lubricant. Discs were formed from these

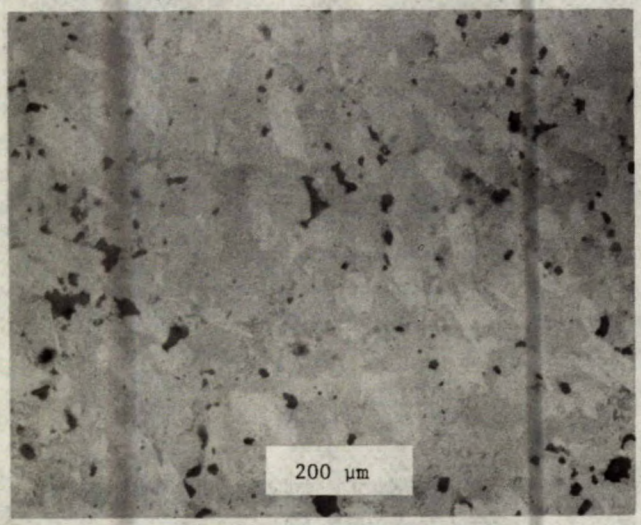

Fig. 23 - Microstructure developed in x = 1.6 nitrate-doped material after firing at 200°C/h to 1275°C and holding at that temperature for 5 h

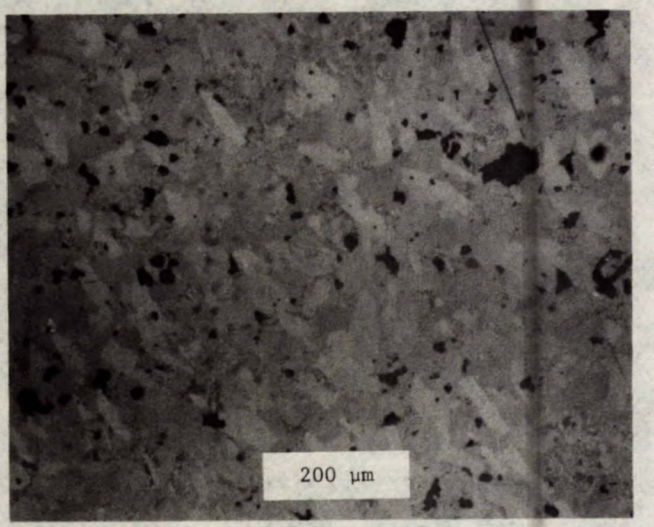

Fig. 25 - Microstructure developed in x = 1.8 nitrate-doped material after fiting at 200°C/h to 1275°C and holding at that temperature for 5 h

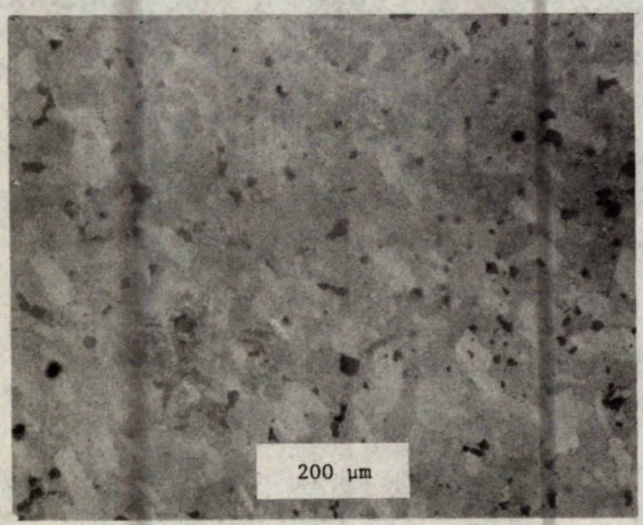

Fig. 24 - Microstructure developed in x = 1.7 nitrate-doped material after firing at 200°C/h to 1275°C and holding at that temperature for 5 h

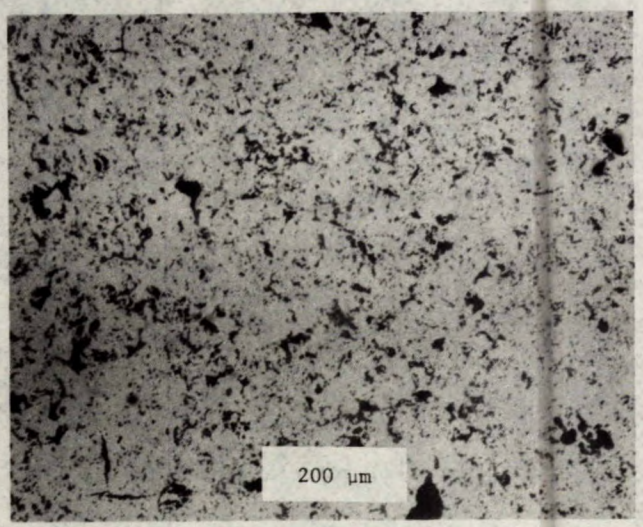

Fig. 26 - Microstructure developed in x = 1.9 nitrate-doped material after firing at 200°C/h to 1275°C and holding at that temperature for 5 h

powders by uniaxially pressing under 70 MPa followed by isostatically pressing at 210 MPa prior to sintering.

Typical microstructures developed in bodies produced using milled powders are shown in Fig. 27 to 33. In essence, the microstructures of both the acetate- and nitrate-doped materials were similar to those developed in sintered bodies produced from unmilled powders. However, the milling step generally resulted in less porosity and also in finer pores. There was also a difference in the grain size and this was particularly pronounced for the nitrate-based material in which x = 1.6 shown in Fig. 23 and 31. The apparently much higher porosity seen in Fig. 31 is misleading as it resulted from a corrosion reaction discussed below; that porosity was not present in the as-fired material.

In both series of materials, second-phase $KHCO_3$ was detected by XRD analysis and was also seen in polished sections at grain boundaries and on the internal surface of what appeared to be isolated pores. However, it is clear that this phase was not present in the material during the firing cycle, otherwise it would have dissolved parts of the compact to form a liquid phase that would gradually crystallize during cooling to leave large well-defined crystals of perhaps a new phase; no such crystalline areas were observed. The gradual formation of $KHCO_3$ on the surface of reduced-fired material of related composition had been noted in previous work by the authors (7). In that case, firing in an H_2 atmosphere resulted in the precipitation of 0.5-μm zones of K_2O throughout the materials; where these intersected the surface, first KOH and then $KHCO_3$ were formed as water vapour and CO_2 were adsorbed from the atmosphere.

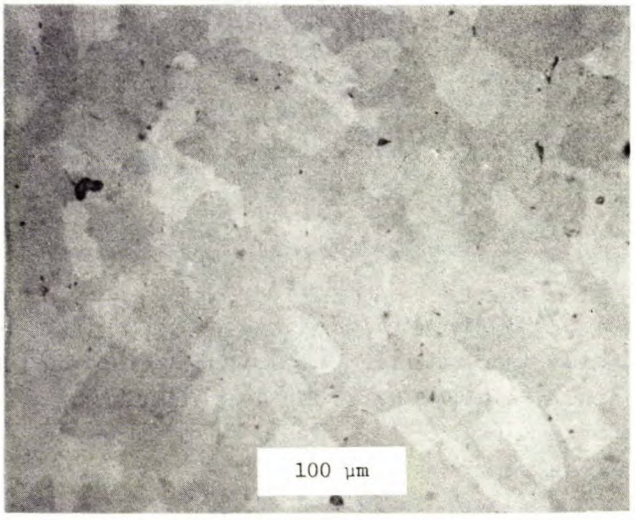

Fig. 27 - Microstructure developed in x = 1.6 acetate-doped material with additional milling after firing at 200°C/h to 1275°C and holding at that temperature for 3 h

In the present work, no K_2O precipitates were detected in any of the fully oxidized compositions, yet the presence of $KHCO_3$ on polished sections was strong evidence that this phase formed on that surface after the polishing stage; $KHCO_3$ could only be detected on the surfaces of these materials after polishing and open storage for at least three months.

In a study of the polishing of sapphire substrates for electronic applications, it was noted that the polishing agent Syton*, which is a stabilized alkaline silica sol, allowed the generation of surface temperatures up to 400°C that resulted in the formation of the compound $Al_2O_3.2SiO_2.2H_2O$ (10). Similar temperatures were doubtless generated in polishing the hollandites and presumably a chemical reaction also occurred at the polished surface. In particular, it is postulated that an ion-exchange reaction occurred that resulted in the formation of K^+-depleted surface layer as possibly NH_4^+ ions from the Syton used in the present work entered the structure. With time, the concentration of K^+ ions at the surface rises as equilibrium is gradually established by the migration of K^+ ions from the bulk of the material to the surface. However, that migration will occur in selected areas where the fast-conducting direction of each crystal, the c-axis, happens to intercept the polished surface perpendicularly; very little migration will occur in those areas where the c-axes happen to lie parallel to the surface. In this manner,

*Available from Monsanto Canada Ltd., Toronto, Ontario

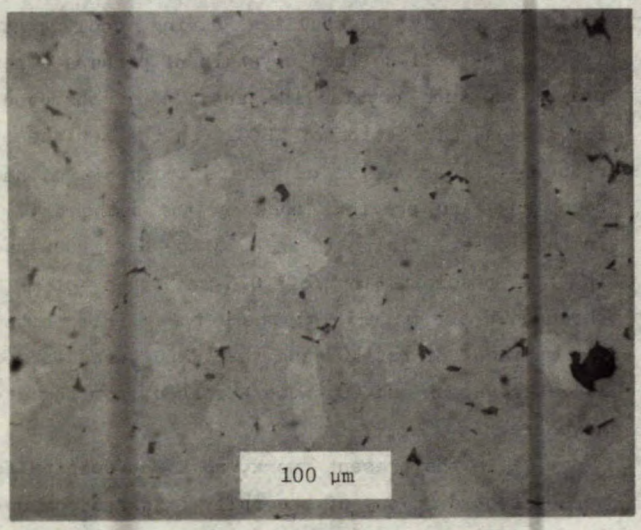

Fig. 28 - Microstructure developed in x = 1.7 acetate-doped material with additional milling after firing at 200°C/h to 1275°C and holding at that temperature for 3 h

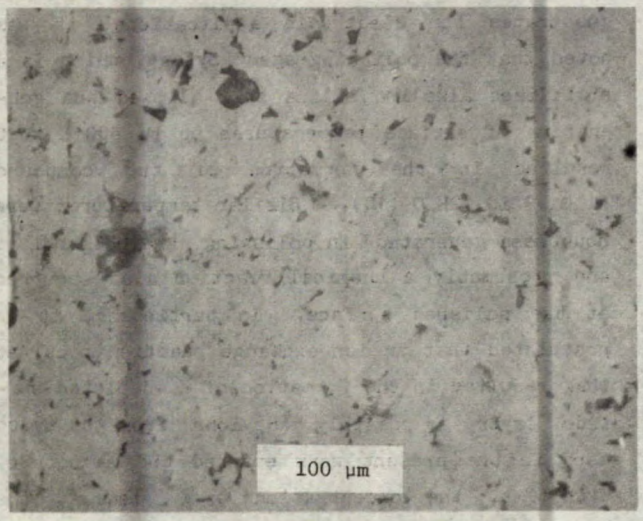

Fig. 29 - Microstructure developed in x = 1.8 acetate-doped material with additional milling after firing at 200°C/h to 1275°C and holding at that temperature for 3 h

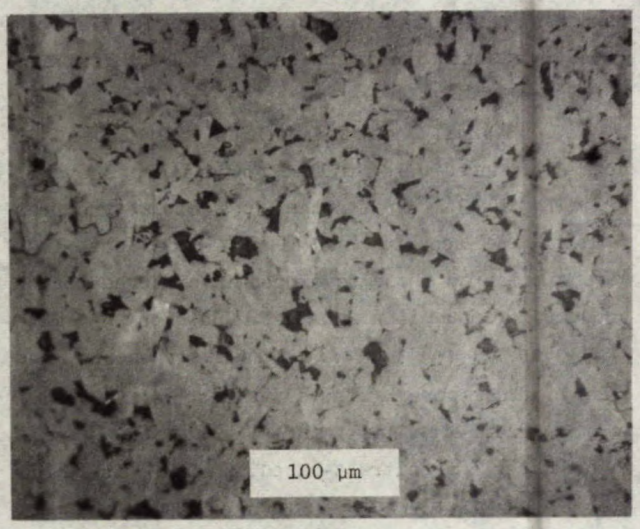

Fig. 30 - Microstructure developed in x = 1.9 acetate-doped material with additional milling after firing at 200°C/h to 1275°C and holding at that temperature for 3 h; showing $KHCO_3$ deposits at grain boundries and in micropores

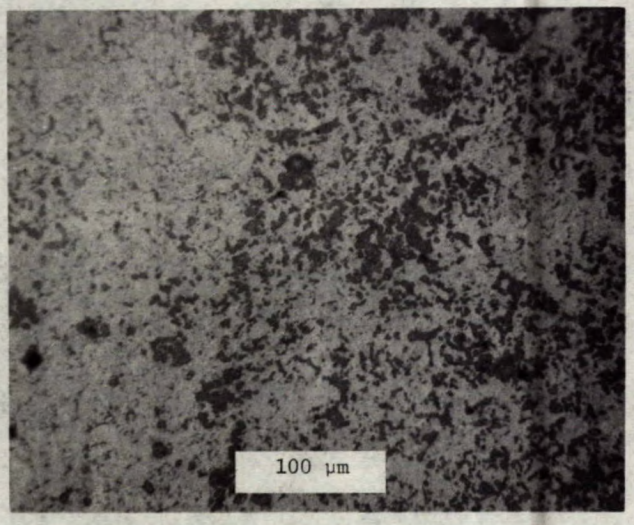

Fig. 31 - Microstructure developed in x = 1.6 nitrate-doped material with additional milling after firing at 200°C/h to 1275°C and holding at that temperature for 3 h; showing $KHCO_3$ deposits at grain boundaries

although an overall equilibrium is developed, there is a considerable difference in the K^+-ion concentration in local areas of the polished surface and this leads to the formation of KOH and $KHCO_3$. As a result of continued exposure to the normal atmosphere, these highly deliquescent pro-

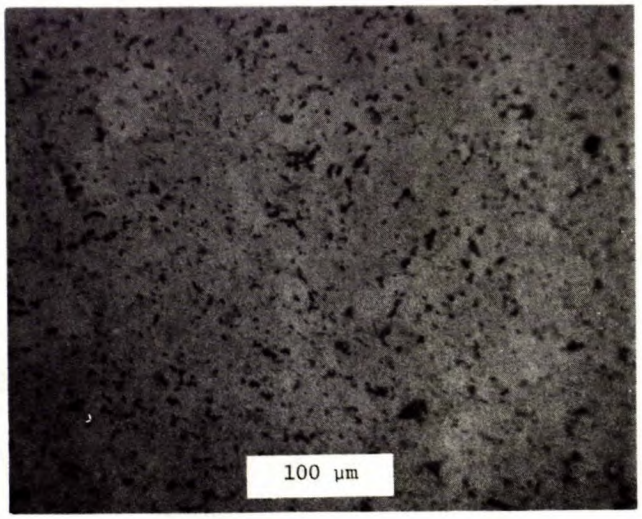

Fig. 32 - Microstructure developed in x = 1.8 nitrate-doped material with additional milling after firing at 200°C/h to 1275°C and holding at that temperature for 3 h, showing the lath-shaped crystals of hollandite being etched out by $KHCO_3$

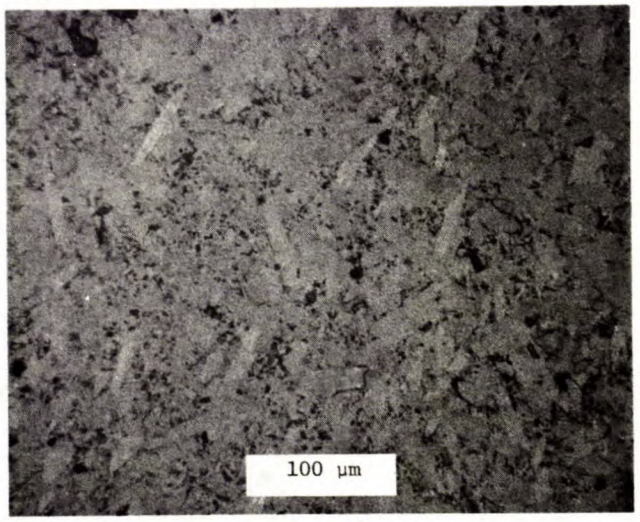

Fig. 33 - Microstructure developed in x = 1.7 nitrate-doped material with additional milling fired at 200°C/h to 1275°C and held at that temperature for 3 h, showing $KHCO_3$ deposits at grain boundaries.

ducts form a concentrated solution on the surface and it is this corrosive liquid that destroys the surface at selected points. It is this mechanism that is believed responsible for the development of the very high apparent porosity seen in Fig. 31. It is important to note that the density of the sample shown in that figure was far too great for the amount of porosity to be representative of the microstructure of the as-fired material. In addition, subsequent work showed that this progressive degradation of the polished surfaces did not occur when the sections were polished using loose diamond powder on a lead lap and a thin mineral-oil lubricant, i.e., when the polishing conditions precluded any ion-exchange reactions.

CONCLUSIONS

It has been shown possible to produce highly reactive, homogeneous raw materials having the general composition: $K_xAl_xTi_{8-x}O_{16}$ by doping freshly precipitated $Ti(OH)_4$ with soluble nitrates or acetates, followed by spray freezing and freeze drying. Using these materials it has been established that the solid-solution limits for the formation of single-phase hollandite are from x = 1.6 to a value between 1.8 and 1.9. At higher values of x, a second phase, isostructural with $K_3Ti_6O_{13}$, is formed and at lower values of x, free TiO_2 is formed.

Although both nitrates and acetates yield reactive materials, it was found that the very high sensitivity of these compositions to the reduction of Ti^{4+} to Ti^{3+}, coupled with the difficulty in ensuring the complete removal of residual carbon on heating the acetate-derived materials, resulted in the development of a two-phase material when compositions in which x = 1.8 and 1.9 were sintered. This effect was further enhanced by the use of carbon-containing organic pressing aids added to both series of materials.

Despite the use of a wet-chemical method for the production of these homogeneous materials, each composition still undergoes a complex reaction path during calcination prior to developing single-phase hollandite. For example, on heating the compositions x = 1.6, 1.7 and 1.8 the following reactions occur in acetate-doped materials:

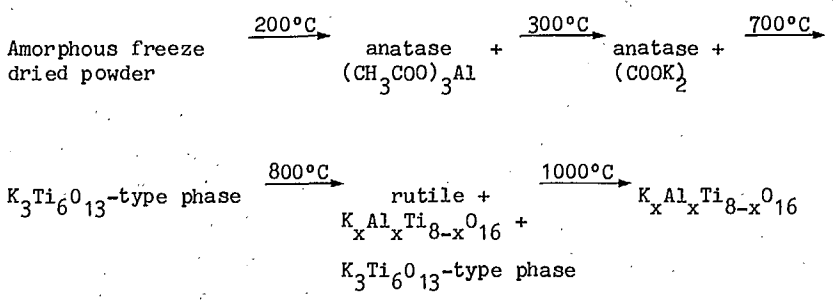

A similar reaction sequence occurs in the nitrate-doped materials, in which KNO_3 is formed at 200°C replacing $(CH_3COO)_3Al$ and $K_3Ti_6O_{13}$-type material is formed at 600 instead of 700°C shown in the above sequence. However, despite this complex reaction path, homogeneous material is formed on firing above 1000°C.

A major difference between the acetate and nitrate-doped raw materials was shown by their differing response to both time and temperature of sintering and the effect these variables had on the sintered density. The acetate-based powders were found to be very sensitive to both these parameters whereas the nitrate-based materials showed a wide tolerance. Both series of materials developed a similar grain size on sintering and both showed a gradual transition of the crystal morphology from an anhedral to a euhedral form with increasing values of x.

The most important processing parameter for the production of an ionically conducting but electronically insulating material was shown to be the sintering atmosphere. The use of an air atmosphere was found to be inadequate to ensure that a fully oxidized and hence electronically insulating product was developed, especially in the TiO_2-rich compositions in which x = 1.6. A synergistic effect was found between the oxygen concentration and the water content of the furnace atmosphere: the higher the water content of the gas, the lower could be the flux rate of oxygen used. However there was a limit, for the use of wet air was found inadequate to fully oxidize compositions in which x = 1.6 and 1.7.

ACKNOWLEDGEMENTS

The authors wish to thank those members of the Mineral Processing Laboratory and of other laboratories who contributed to this report, Thanks are particularly due to A.J. Hanson who conducted much of the technical and processing aspects, to H.J.C. Childe for X-ray diffraction analyses and to G. Lemieux for thermal analyses.

REFERENCES

1. Wheat, T.A. "Ionically conducting ceramics and their applications"; J Can Ceram Soc 47:7-15; 1978.

2. Dryden, I.S. and Wadsley, A.D. "Structure and dielectric properties of compounds with the formula $Ba_x(Ti_{8-x}Mg_x)O_{16}$"; Trans Faraday Soc 54:1574-1580; 1958.

3. Takahashi, T. and Kuwabara, K. "Preparation of sintered oxides with a hollandite-type structure ($K_xMg_{x/2}Ti_{8-x}O_{16}$) and their ionic conduction"; Nippon Kagaku Kaishi 10:1883-1887; 1974.

4. Takahashi, T., Kuwabara, K. and Aoyama, H. "Preparation of sintered oxide with a hollandite-type structure ($K_xM_xTi_{8-x}O_{16}$)(M = Al,Fe, Co,Cr) and its ionic conduction"; Chem Soc Japan 12:2291-2296; 1974.

5. Reau, J.M., Moali, J. and Hagenmuller, P. "Etude de la conductivité de solutions sol ides de structure hollandite $K_xM_{x/2}Ti_{8-x}O_{16}$ (M = Mg,Zn) et $K_xAl_xTi_{8-x}O_{16}$"; J Phys Chem Solids 38:1395-1398; 1977.

6. Singer, J., Kautz, H.E., Fielder, W.L. and Fordyce, J.S. "Selection and preliminary evaluation of three structures as potential solid conductors of alkali ions: two hollandites, a titanate and a tungstate"; pp 653-663 in Fast Ion Transport in Solids, Solid State Batteries and Devices, edited by W. Van Gool, published by North American Elsevier, New York, 1973.

7. Quon, H.H. and Wheat, T.A. "Preparation of a ceramic electrolyte in the system $MgO-K_2O-TiO_2$"; CANMET Report 78-8; CANMET, Energy, Mines and Resources Canada; 1977.

8. Gallagher, P.K., Johnson, D.W., Shrey, F. and Nitti, D.J. "Preparation and characterization of iron oxide"; Am Ceram Soc Bull 52:247-250; 1973.

9. MacDonald, W.A., Wheat, T.A. and Quon, H.H. "A method for the rapid mounting and polishing of ceramic materials for microstructural examinations"; J Mater Sci 13:905-905; 1978.

10. Gutsche, H.W. and Moody, J.W. "Polishing of sapphire with colloidal silica"; J Electrochem Soc 125:1:136-138; 1978.

APPENDIX A

DETERMINATION OF QUANTITY OF POTASSIUM AND ALUMINUM ACETATE AND POTASSIUM AND ALUMINUM NITRATE REQUIRED TO PRODUCE SPECIFIC CONCENTRATIONS OF POTASSIUM AND ALUMINUM IN TITANIA

CONCENTRATION OF TITANIA SLURRY

Samples of the slurry were taken from the main batch after washing to remove Cl^- contamination. After vigorous stirring for 2 h, the precipitate was divided into equal portions by transferring into weighed containers. Samples of slurry from each container were taken to determine the titania concentration. In each case, duplicate 25-mL aliquots were withdrawn and placed in weighed Pt dishes that were subsequently dried at 110°C overnight and then ignited to constant mass at 1000°C.

QUANTITY OF EACH ACETATE REQUIRED FOR DOPED SLURRY

From the mass of each batch and the slurry concentration, the quantity of TiO_2 in each separate batch was determined. The example given below illustrates the formulation of a doped titanate having the composition: $0.8K_2O:0.8Al_2O_3:6.4TiO_2$, i.e., where x equals 1.6.

These quantities of each acetate were dissolved in distilled water to give two separate 0.5-molar solutions that were subsequently mixed and slowly added to the vortex of the vigorously stirred slurry.

QUANTITY OF EACH NITRATE REQUIRED FOR DOPED SLURRY

The doping of nitrate in the titania slurry is identical to the acetate doping. The example given below illustrates the formulation of a doped titanate having the composition: $0.85K_2O:0.85Al_2O_3:6.3TiO_2$, i.e., where x equals 1.7.

These quantities of each nitrate were dissolved in distilled water in the same manner as described for doping of the acetate titanate.

Table A-1 - Determination of titania concentration in slurry

		Sample 1	Sample 2
Mass of slurry (g)	=	24.8915	24.8480
Mass of TiO_2 formed (g)	=	0.5331	0.5411
Concentration of slurry (g TiO_2/g slurry)	=	0.02142	0.02177
Average concentration of slurry (g TiO_2/g slurry)	=	0.02159	

Table A-2 - Determination of quantity of potassium and aluminium acetates required to produce the composition x = 1.6

Mass TiO_2 g	Mole TiO_2	Need mole K_2O	Need mole Al_2O_3	Need mole K.Ac*	Need mole basic Ac.*	Mass K.Ac needed g	Mass Al basic Ac needed g
95.4784	1.19499	0.14937	0.14937	0.29874	0.29874	29.3183	60.9728

*Ac: acetate group, i.e., $CH_3.COO^-$

Table A-3 - Determination of quantity of potassium and aluminium nitrates required to produce the composition x = 1.7

Mass TiO_2 g	Mole TiO_2	Need mole K_2O	Need mole Al_2O_3	Need mole K.N*	Need mole Al.N**	Mass KN needed g	Mass Al.N needed g
168.55	2.10951	0.28462	0.28462	0.56923	0.56923	58.0276	213.5420

*KN = KNO_3, **Al.N = $Al(NO_3)_3.9H_2O$

APPENDIX B

COLOUR AND BULK DENSITY OF ACETATE- AND NITRATE-DOPED MATERIALS CONTAINING GELVA V-7 AND CARBOWAX 400 ADDITIVES

In all cases, samples were first formed into cylinders by uniaxially pressing at 70 MPa prior to isostatically pressing at 210 MPa to develop the green densities reported in Tables B-1 and B-2. The discs produced were subsequently fired in wet oxygen.

Table - B-1 - Green and fired bulk densities and fired colour of acetate-doped titanates containing Gelva V-7 binder and Carbowax 400 lubricant

	Green					Fired					
Composition	Diameter cm	Thickness cm	Mass g	Density kg/m^3	Average density kg/m^3	Diameter cm	Thickness cm	Mass g	Density kg/m^3	Average density kg/m^3	Colour*
1.6	3.531	1.021	20.6718	2230		2.799	0.800	18.2141	3686		G
	3.406	1.016	20.4851	2210		2.591	0.823	18.2632	3630		SG
	3.432	0.381	7.9252	2250	2230	2.814	0.323	6.9809	3480	3629	G
	3.434	0.371	7.6430	2230		2.822	0.292	6.8029	3720		C
1.7	3.416	0.978	20.0395	2240		2.808	0.787	18.1695	3730		SG
	3.421	1.008	20.7129	2240		2.819	0.808	18.2445	3620		C
	3.442	0.343	7.1754	2250	2245	2.832	0.272	6.3154	3690	3685	SG
	3.434	0.378	7.8747	2250		2.824	0.299	6.9427	3700		C
1.8	3.368	1.029	19.8603	2170		2.788	0.622	18.1717	3610		C
	3.373	1.049	20.4239	2180		2.784	0.838	18.2993	3590		C
	3.383	0.384	7.5597	2190	2180	2.789	0.310	6.7722	3580	3616	C
	3.399	0.330	6.5440	2190		2.896	0.259	5.8400	3680		C
	3.437	0.345	6.9478	2170		2.807	0.277	6.1943	3620		C
1.9	3.444	0.929	20.2182	2340		2.930	0.745	17.2356	3420		C
	3.454	0.899	19.6589	2330	2335	2.908	0.767	17.7600	3490	3520	C
	3.454	0.351	7.6871	2340		2.908	0.287	6.7767	3550		C
	3.467	0.343	7.5406	2330		2.987	0.277	6.1943	3620		C

*G = grey SG = slight grey C = cream

Table - B-2 - Green and fired bulk densities and fired colour of nitrate-doped titanates containing Gelva V-7 binder and Carbowax 400 lubricant

	Green					Fired					
Composition	Diameter cm	Thickness cm	Mass g	Density kg/m^3	Average density kg/m^3	Diameter cm	Thickness cm	Mass g	Density kg/m^3	Average density kg/m^3	Colour*
1.6	3.4823	0.892	19.9090	2340		2.9970	0.762	18.1456	3390		C
	3.4798	0.899	19.9219	2330		2.9640	0.772	18.1800	3410		G
	3.4645	0.884	19.5776	2350		2.9590	0.749	17.8287	3460		C
	3.4620	0.902	19.8671	2340	2321	3.0050	0.772	18.1076	3310	3417	C
	3.5052	0.906	20.0153	2300		3.0963	0.785	19.0051	3470		C
	3.5052	0.909	20.1066	2290		2.9921	0.775	19.0438	3500		C
	3.4950	0.909	20.0770	2300		3.0200	0.785	18.9819	3380		C
1.7	3.4188	0.958	20.0574	2280		2.8981	0.805	19.0020	3580		C
	3.4366	0.940	20.0202	2300		2.9460	0.800	19.0276	3490		C
	3.4265	0.953	20.0209	2300		2.9930	0.805	18.9916	3590		C
	3.4620	0.932	20.1553	2300	2301	2.9360	0.797	19.0380	3530	3546	C
	3.4925	0.909	20.1492	2310		2.9972	0.772	19.0899	3500		C
	3.4976	0.920	20.4307	2310		2.9743	0.780	19.3586	3570		C
	3.5001	0.922	20.5235	2310		2.9921	0.780	19.4948	3560		C
1.8	3.3960	0.970	20.3177	2310		2.8851	0.818	19.2165	3600		C
	3.4265	0.930	19.9283	2320		2.9492	0.800	18.9440	3470		C
	3.4040	0.942	20.2393	2361		2.8854	0.795	18.9772	3640		C
	3.4034	0.950	20.0281	2320	2350	2.8850	0.813	18.9636	3570	3560	C
	3.4976	0.884	20.1864	2380		3.0023	0.749	18.8233	3550		C
	3.5052	0.864	19.8684	2380		3.0048	0.734	18.3204	3520		C
	3.5128	0.887	20.4735	2380		3.0099	0.754	19.1502	3570		C

*C = cream G = grey

OPINION POLL

The opinion of concerned readers may influence the direction of future CANMET research.

We invite your assessment of this report - No._____

Is it useful?	Yes_____	No_____
Is it pertinent to an industry problem?	Yes_____	No_____
Is the subject of high priority?	Yes_____	No_____

Comments_____

_____

_____

Please mail to: CANMET Editor, EMR, 555 Booth Street,
Ottawa, Ontario, K1A 0G1

A complimentary copy of the CANMET REVIEW describing CANMET research activity will be sent on request.

CANMET REPORTS

Recent CANMET reports presently available or soon to be released through Printing and Publishing, Supply and Services, Canada (addresses on inside front cover), or from CANMET Publications Office, 555 Booth Street, Ottawa, Ontario, K1A 0G1:

Les récents rapports de CANMET, qui sont présentement disponibles ou qui le seront bientôt peuvent être obtenus de la direction de l'Imprimerie et de l'Edition, Approvisionnements et Services Canada (adresses au verso de la page couverture), ou du Bureau de vente et distribution de CANMET, 555, rue Booth, Ottawa, Ontario, K1A 0G1:

79-8 Flotation techniques for producing high-recovery bulk Zn-Pb-Cu-Ag concentrate from a New Brunswick massive sulphide ore; A.I. Stemerowicz and G.W. Leigh;
Cat. No. M38-13/79-8, ISBN 0-660-10448-2; Price: $8.00 Canada, $9.60 other countries.

79-10 A comparative study of lightweight aggregates in structural concrete; H.S. Wilson;
Cat. No. M38-13/79-10, ISBN 0-660-10449-0; Price: $2.00 Canada, $2.40 other countries.

79-11 CANMET's rock mechanics research at the Kid Creek mine; D.G.F. Hedley, G. Herget, P. Miles and Y.S. Yu;
Cat. No. M38-13/79-11, ISBN 0-660-10472-5; Price: $3.50 Canada, $4.20 other countries.

79-17 Rapid chromatographic procedure for characterizing hydrocarbons in synthetic fuel naphtha; A.E. George, G.T. Smiley and H. Sawatzky;
Cat. No. M38-13/79-17, ISBN 0-660-10428-8; Price: $2.75 Canada, $3.30 other countries.

79-18 Influence of flue temperature and coal preparation on coke quality in 460-mm technical scale coke oven; J.F. Gransden and W.R. Leeder;
Cat. No. M38-13/79-18, ISBN 0-660-10441-5; Price: $1.50 Canada, $1.80 other countries.

79-20 Effect of hydrocracking on the distribution of nitrogenous components in Athabasca bitumen; H. Sawatzky, J.E. Beshai, G.T. Smiley and A.E. George;
Cat. No. M38-13/79-20, ISBN 0-660-10442-3; Price: $1.25 Canada, $1.50 other countries.

79-25 CANMET review 1978-79; Staff of CANMET;
Cat. No. M38-13/79-25, ISBN 0-660-10522-5; Price: $4.25 Canada, $5.10 other countries.

79-28 Sulphur concrete and sulphur infiltrated concrete: Properties, applications and limitations; V.M. Malhotra;
Cat. No. M38-13/79-28, ISBN 0-660-10469-5; Price: $2.25 Canada, $2.70 other countries.

79-29 Geological disposal of high-level radioactive wastes; D.F. Coates, G. Larocque and L. Geller; (Policy paper);
Cat. No. M38-13/79-29, ISBN 0-660-10523-3; Price: $1.50 Canada, $1.80 other countries.

79-30 In situ testing for concrete strength; V.M. Malhotra and G.G. Carette;
Cat. No. M38-13/79-30, ISBN 0-660-10506-3; Price: $1.75 Canada, $2.10 other countries.

79-31 Superplasticizers: Their effect on fresh and hardened concrete; V.M. Malhotra;
Cat. No. M38-13/79-31, ISBN 0-660-10530-6; Price: $2.00 Canada, $2.40 other countries.

79-32 Concrete made with supplementary cementing materials; E.E. Berry;
Cat. No. M38-13/79-32, ISBN 0-660-10470-9; Price: $2.25 Canada, $2.70 other countries.

79-33 Lightweight aggregates: Properties, applications and outlook; H.S. Wilson;
Cat. No. M38-13/79-33, ISBN 0-660-10482-2; Price: $2.25 Canada, $2.70 other countries.